Synchrophasor and Frequency Estimations: Combining Space Vector and Taylor-Fourier Approaches

Paolo Castello*, Roberto Ferrero†, Paolo Attilio Pegoraro*, Sergio Toscani‡

*Department of Electrical and Electronic Engineering, University of Cagliari, Cagliari, Italy
Email: [paolo.castello, paolo.pegoraro]@diee.unica.it

†Department of Electrical Engineering and Electronics, University of Liverpool, Liverpool, UK
Email: roberto.ferrero@liverpool.ac.uk

‡Dipartimento di Elettronica, Informazione e Bioingegneria, Politecnico di Milano, Milan, Italy
Email: sergio.toscani@polimi.it

***Abstract*—Taylor-Fourier (TF) filters represent a powerful tool to design PMU algorithms able to estimate synchrophasor, frequency and rate of change of frequency (ROCOF). The resulting techniques are based on dynamic representations of the synchrophasor, hence they are particularly suitable to track the evolution of its parameters during time-varying conditions. Electrical quantities in power systems are typically three-phase and weakly unbalanced, but most PMU measurement techniques are developed by considering them as a set of three single phase signals; on the contrary, this peculiarity can be favorably exploited. For the first time, in this paper, the TF approach is applied to the space vector obtained from three-phase measurements. The positive sequence synchrophasor can be easily extracted along with the system frequency and ROCOF leveraging the three-phase characteristics. Performance of the proposed technique is assessed by using test signals defined by the standard IEEE C37.118.1-2011. Results show that the positive sequence estimations are always more accurate when compared to the single-phase measurements provided by the conventional TF algorithms under the same conditions.**

***Index Terms*—Phasor Measurement Unit (PMU), Synchrophasor estimation, Frequency, Rate of Change of Frequency (ROCOF), Voltage Measurement.**

I. Introduction

Phasor Measurement Units (PMUs) are synchronized devices intended to measure amplitude, phase angle, frequency and rate of change of frequency (ROCOF) of electrical signals in power networks. Initially designed for transmission networks [1], they are expected to become a widespread tool also for electric distribution systems, being considered as fundamental to pave the implementation of smart grids [2] able to automatically control the network operation based on accurate, fast and reliable monitoring.

PMUs label data with time-tags referred to a common timescale (the coordinated universal time, UTC, obtained from a GPS receiver is typically adopted), so that measurements collected on a wide area can be correlated and used even in real-time, thus enabling an accurate representation of the operating conditions that can be exploited in network control applications [2].

PMU algorithms are designed to extract the fundamental frequency component, along with the corresponding frequency and ROCOF, coping with different conditions that may occur in electrical signals: dynamics, harmonic and interharmonic disturbances, rapid variations, etc.

Several algorithms have been proposed in recent literature (see [3] for a review). The proposed algorithms cover a wide range of estimation techniques and specific testing conditions. Signal dynamics is particularly important, since PMUs are designed to operate even at high reporting rates (50 frames/s or higher in 50 Hz systems) in order to track amplitude, phase angle and frequency changes. The last standard for synchrophasor measurements IEEE C37.118.1-2011 [4] (along with its amendment [5]) introduces the definition of dynamic synchrophasor and prescribes specific tests that can be representative of both slow variations, like amplitude or phase angle modulations and linear frequency ramps, and abrupt changes, such as amplitude and phase angle steps. For each test, upper limits for the accuracy or the dynamic response of PMUs are reported.

An interesting approach to measure dynamic signal parameters was proposed in [6] where a Taylor expansion of the phasor around the measurement instant is adopted to better describe its time evolution, thus allowing a more accurate dynamic tracking of the related quantities. Such model has been exploited by different algorithms. In [7], [8], for instance, estimations are based on the discrete Fourier transform (DFT) and the model is employed to correct them by considering the effects due to parameter variations. In [9] the Taylor expansion approach is used to extend the interpolated DFT algorithm, while in [10] a two-channel PMU algorithm based on a Taylor approach is employed to design a PMU that is simultaneously compliant with requirements of P and M classes defined by [4], [5].

All the above algorithms are designed starting from a single-phase signal. Recently, the idea of exploiting the characteristics of three-phase quantities to define PMU algorithms has been

proposed. In particular, in [11] a space vector (SV) based algorithm is introduced. The positive sequence synchrophasor is obtained from the SV by means of an IIR filtering stage and two least squares FIR interpolators: a first one for amplitude estimation and a second one allowing phase angle and frequency measurements. In [12], all the quantities are derived by FIR filtering the real and imaginary parts of the SV, and, in particular, frequency and ROCOF are obtained by applying properly-designed first and second order partial-band FIR differentiators, respectively, which allow designing algorithms that are compliant with the performance classes defined in [4] and [5]. In [13], the SV transformation is considered as a preliminary stage for the Interpolated DFT computation, thus allowing better estimations in the presence of off-nominal frequency conditions.

In this paper, a new algorithm is proposed, which is the combination of the above approaches. It applies the Taylor expansion model to the SV, thus permitting the estimation of the positive-sequence synchrophasor, frequency and ROCOF that characterize three-phase signals.

II. Background and proposed approach

PMU algorithms apply to three-phase signals, which can be written as follows:

$$\boldsymbol{x}_{abc}(t) = \begin{bmatrix} x_a(t) \\ x_b(t) \\ x_c(t) \end{bmatrix} \tag{1}$$

where $x_p(t)$ ($p \in \{a,b,c\}$) represents the generic phase voltage or current signal. If sinusoidal steady-state conditions hold, signals can be represented by their respective phasors $\bar{X}_a$, $\bar{X}_b$, $\bar{X}_c$:

$$\boldsymbol{X}_{abc} = \begin{bmatrix} \bar{X}_a \\ \bar{X}_b \\ \bar{X}_c \end{bmatrix} = \begin{bmatrix} X_a e^{j\varphi_a} \\ X_b e^{j\varphi_b} \\ X_c e^{j\varphi_c} \end{bmatrix} \tag{2}$$

where the phase angles are referred to a common time axis. An alternative representation in terms of positive-, negative- and zero-sequence components can be obtained by applying the well-known, bijective Fortescue transformation ($\bar{\alpha} \triangleq e^{j2\pi/3}$):

$$\begin{bmatrix} \bar{X}_+ \\ \bar{X}_- \\ \bar{X}_0 \end{bmatrix} = \begin{bmatrix} X_+ e^{j\varphi_+} \\ X_- e^{j\varphi_-} \\ X_0 e^{j\varphi_0} \end{bmatrix} = \frac{1}{\sqrt{3}} \begin{bmatrix} 1 & \bar{\alpha} & \bar{\alpha}^2 \\ 1 & \bar{\alpha}^2 & \bar{\alpha} \\ 1 & 1 & 1 \end{bmatrix} \boldsymbol{X}_{abc} \tag{3}$$

Generalizing the phasor concept, the dynamic synchrophasor can be defined as the complex value representing the instantaneous amplitude and phase angle measured with respect to a common time reference (typically UTC). For instance, when a sinusoidal signal with off-nominal frequency $f_1 \neq f_0$ is considered, we get:

$$\bar{X}_p(t) = X_p e^{j\varphi_p(t)} = X_p e^{j(\omega_1 t + \varphi_{p0})} \tag{4}$$

where $p \in \{a,b,c\}$ and $\omega_1 = 2\pi f_1$. For a generic time-varying frequency, $\varphi_p(t)$ in (4) includes the time integral of the instantaneous angular frequency contributions. The definition of the dynamic synchrophasor given in [4] refers to measurements obtained at fixed reporting instants that are multiples of $T_0 = 1/f_0$. According to this, the generic synchrophasor phase-angle $\varphi'_p(t)$ results:

$$\varphi'_p(t) = \varphi_p(t) - 2\pi f_0 t = \int_0^t \omega_1(\tau) d\tau + \varphi_{p0} - 2\pi f_0 t \tag{5}$$

and thus considers the wrapping of the angle rotating at nominal frequency that occurs at $t = kT_0$. To avoid possible misunderstandings when a generic reporting interval T_{RR} (e.g, T_{RR} equal to the sampling time T_s) is considered, in the following, the synchrophasor phase-angle $\varphi_p(t)$ will be used.

With the above definitions, the time domain signals in an interval around the generic reporting instant t_r can be represented as:

$$\boldsymbol{x}_{abc}(t) = \frac{1}{\sqrt{2}} \left(\begin{bmatrix} \bar{X}_a(t_r) \\ \bar{X}_b(t_r) \\ \bar{X}_c(t_r) \end{bmatrix} e^{j\omega_1(t-t_r)} + \begin{bmatrix} \bar{X}^*_a(t_r) \\ \bar{X}^*_b(t_r) \\ \bar{X}^*_c(t_r) \end{bmatrix} e^{-j\omega_1(t-t_r)} \right) \tag{6}$$

Similar considerations hold for the positive sequence synchrophasor $\bar{X}_+(t)$. It is important to recall that a PMU is required to measure also the instantaneous frequency $f_1(t)$ and ROCOF $R(t)$, and that such quantities are shared by all the phases of the system. For this reason, the space vector approach summarized in the following is well-suited for the design of measurement algorithms.

A. Space Vector Based Approach

PMU algorithms based on the SV transformation have been recently proposed by the authors in [11], [12]. The underlying idea is to exploit the properties of electrical signals in three-phase systems to perform synchrophasor, frequency and ROCOF estimations using the (complex) SV signal:

$$\bar{x}_{SV}(t) = x_d(t) + j x_q(t) = \sqrt{\frac{2}{3}} \begin{bmatrix} 1 & \bar{\alpha} & \bar{\alpha}^2 \end{bmatrix} \boldsymbol{x}_{abc}(t) e^{-j\beta(t)} \tag{7}$$

where $\beta(t)$ is the angular position of the rotating reference frame (in the following it will be considered equal to zero).

Substituting (6) and the inverse of (3) into (7) it is possible to express the SV in terms of symmetrical components:

$$\bar{x}_{SV}(t - t_r) = \bar{X}_+(t_r) e^{j\omega_1(t-t_r)} + \bar{X}^*_-(t_r) e^{-j\omega_1(t-t_r)} \tag{8}$$

From (8), it is clear that the SV is unaffected by the zero sequence term, while the negative sequence component appears as a harmonic disturbance characterized by a negative angular frequency $-\omega_1$.

Thanks to (8), the impact of the image component on the synchrophasor estimation is largely reduced when the positive sequence synchrophasor estimation is considered, since in this case the negative frequency component only depends on unbalance. Transmission networks typically show weak unbalance, while in distribution systems higher levels can be

found. It is important to notice that even extreme unbalance conditions, such as the absence of one phase signal, result in negative sequences which are considerably lower than the positive ones [14]. These considerations suggest applying phasor, frequency and ROCOF estimation techniques directly to the SV to improve the estimation.

B. Taylor-Fourier Approach

In the Taylor-Fourier filtering approach introduced in [6] the synchrophasor dynamics is modeled by means of a Taylor expansion of its real and imaginary parts around the measurement instant:

$$\bar{X}_p(t-t_r) = \sum_{k=0}^{K} \bar{X}_p^{(k)}(t_r)\frac{(t-t_r)^k}{k!} \tag{9}$$

where $\bar{X}_p^{(k)}(t_r)$ is the kth derivative of the synchrophasor ($k = 0$ indicates the phasor itself) at t_r, and K is the expansion order. Then, for the samples in a N-size window centered on t_r (N odd from here on for the sake of simplicity), the following relationship holds true:

$$\mathbf{x}_p(t_r) = \frac{1}{\sqrt{2}}\left[\mathbf{\Phi A} \;\; \mathbf{\Phi}^{\mathsf{H}}\mathbf{A}\right]\cdot \mathbf{p}_p(t_r) = \frac{1}{\sqrt{2}}\mathbf{B}\cdot\mathbf{p}_p(t_r) \tag{10}$$

where $^{\mathsf{H}}$ indicates the Hermitian operator ($^{\mathsf{T}}$ is the transpose) and:

$$\mathbf{x}_p(t_r) = \begin{bmatrix} x_p(t_r + \frac{N-1}{2}T_s) \\ \vdots \\ x_p(t_r) \\ \vdots \\ x_p(t_r - \frac{N-1}{2}T_s) \end{bmatrix} \tag{11}$$

$$\mathbf{p}_p(t_r) = \left[\bar{X}_p^{(0)}(t_r), \cdots, \bar{X}_p^{(K)}(t_r), \bar{X}_p^{(0)*}(t_r), \cdots, \bar{X}_p^{(K)*}(t_r)\right]^{\mathsf{T}} \tag{12}$$

$$\mathbf{A} = \begin{bmatrix} 1 & \frac{N-1}{2}T_s & \frac{\left(\frac{N-1}{2}T_s\right)^2}{2} & \cdots & \frac{\left(\frac{N-1}{2}T_s\right)^K}{k!} \\ \vdots & \vdots & \vdots & & \vdots \\ 1 & 0 & 0 & & 0 \\ \vdots & \vdots & \vdots & & \vdots \\ 1 & -\frac{N-1}{2}T_s & \frac{\left(-\frac{N-1}{2}T_s\right)^2}{2} & \cdots & \frac{\left(-\frac{N-1}{2}T_s\right)^K}{k!} \end{bmatrix} \tag{13}$$

$$\mathbf{\Phi} = \begin{bmatrix} e^{j\omega_0\frac{N-1}{2}T_s} & & & & \\ & \ddots & & & \\ & & 1 & & \\ & & & \ddots & \\ & & & & e^{-j\omega_0\frac{N-1}{2}T_s} \end{bmatrix} \tag{14}$$

From (10), the estimation of the synchrophasor along with its K derivatives is obtained by means of a weighted least squares (WLS) approach as $\hat{\mathbf{p}}_p(t_r) = \sqrt{2}(\mathbf{B}^{\mathsf{H}}\mathbf{B})^{-1}\mathbf{B}^{\mathsf{H}}\cdot\mathbf{x}_p(t_r) = \sqrt{2}\mathbf{H}\cdot\mathbf{x}_p(t_r)$. The estimation is thus linear and corresponds to a bank of FIR filters of length N (the rows of matrix $\sqrt{2}\mathbf{H}$), one for each derivative order, applied to the input signal.

Frequency and ROCOF are estimated exploiting the first and second order phasor derivatives ($K = 2$ is typically chosen) with the following formulas:

$$\Delta\hat{f}(t_r) = \frac{1}{2\pi}\frac{\Im\left[\hat{\bar{X}}_p^{(1)}(t_r)\cdot\hat{\bar{X}}_p^{(0)*}(t_r)\right]}{\left|\hat{\bar{X}}_p^{(0)}(t_r)\right|^2} \tag{15}$$

$$\widehat{\mathrm{ROCOF}}(t_r) = \frac{1}{\pi}\left(\frac{\Im\left[\hat{\bar{X}}_p^{(2)}(t_r)\bar{X}_p^{(0)*}(t_r)\right]}{2\left|\hat{\bar{X}}_p^{(0)}(t_r)\right|^2} + - \frac{\Re\left[\hat{\bar{X}}_p^{(1)}(t_r)\hat{\bar{X}}_p^{(0)*}(t_r)\right]\Im\left[\hat{\bar{X}}_p^{(1)}(t_r)\hat{\bar{X}}_p^{(0)*}(t_r)\right]}{\left|\hat{\bar{X}}_p^{(0)}(t_r)\right|^4}\right) \tag{16}$$

where $\Delta f(t_r) = f_1(t_r) - f_0$ is the frequency deviation with respect to the nominal one while '$\hat{}$' denotes the estimated quantities.

C. Proposed Technique: Combining Space Vector and Taylor Fourier Approaches

In this paper, the Taylor expansion of the synchrophasor around its measurement instant is applied to the positive and negative sequence components and thus we obtain the equivalent expression of (10) for a sample window $\bar{\mathbf{x}}_{SV}(t_r) = \left[\bar{x}_{SV}(t_r + \frac{N-1}{2}T_s), \cdots, \bar{x}_{SV}(t_r), \cdots, \bar{x}_{SV}(t_r - \frac{N-1}{2}T_s))\right]^{\mathsf{T}}$ of the SV:

$$\bar{\mathbf{x}}_{SV}(t_r) = \left[\mathbf{\Phi A} \;\; \mathbf{\Phi}^{\mathsf{H}}\mathbf{A}\right]\cdot\mathbf{p}_{\pm}(t_r) = \mathbf{B}\cdot\mathbf{p}_{\pm}(t_r) \tag{17}$$

where:

$$\mathbf{p}_{\pm}(t_r) = \left[\bar{X}_+^{(0)}(t_r), \cdots, \bar{X}_+^{(K)}(t_r), \bar{X}_-^{(0)*}(t_r), \cdots, \bar{X}_-^{(K)*}(t_r)\right]^{\mathsf{T}} \tag{18}$$

is the vector of the positive- and negative-sequence synchrophasors along with their derivatives up to order K (referred to the measurement instant t_r).

By means of the WLS computation it is possible to use the filter bank in $\mathbf{H} = (\mathbf{B}^{\mathsf{H}}\mathbf{B})^{-1}\mathbf{B}^{\mathsf{H}}$, as explained above in Section II-B, to estimate $\mathbf{p}_{\pm}(t_r)$. Then, the estimation of the positive sequence synchrophasor, of the frequency deviation with respect to the nominal one, and of the ROCOF is achieved by means of the following equations:

$$\hat{\mathbf{p}}_{\pm}(t_r) = \mathbf{H}\cdot\bar{\mathbf{x}}_{SV}(t_r) \tag{19}$$

$$\hat{\bar{X}}_+(t_r) = \hat{p}_{\pm,1} = \mathbf{H}_{1,*}\cdot\bar{\mathbf{x}}_{SV}(t_r) = \underline{\mathbf{h}}_1^{\mathsf{T}}\cdot\bar{\mathbf{x}}_{SV}(t_r) \tag{20}$$

$$\Delta\hat{f}(t_r) = \frac{1}{2\pi}\frac{\Im\left[\hat{\bar{X}}_+^{(1)}(t_r)\cdot\hat{\bar{X}}_+^{*}(t_r)\right]}{\left|\hat{\bar{X}}_+(t_r)\right|^2} \tag{21}$$

$$\widehat{\mathrm{ROCOF}}(t_r) = \frac{1}{\pi}\left(\frac{\Im\left[\hat{\bar{X}}_+^{(2)}(t_r)\hat{\bar{X}}_+^{*}(t_r)\right]}{2\left|\hat{\bar{X}}_+(t_r)\right|^2} + - \frac{\Re\left[\hat{\bar{X}}_+^{(1)}(t_r)\hat{\bar{X}}_+^{*}(t_r)\right]\Im\left[\hat{\bar{X}}_+^{(1)}(t_r)\hat{\bar{X}}_+^{*}(t_r)\right]}{\left|\hat{\bar{X}}_+(t_r)\right|^4}\right) \tag{22}$$

where the generic vector $\underline{\mathbf{h}}_k^{\mathsf{T}}$ is the left-to-right flipped version of $\mathbf{h}_k^{\mathsf{T}}$, which is the vector of the coefficients of the generic kth-order FIR differentiator. Other than providing the estimates of the positive sequence synchrophasor, the combined method (SV-TF in the following) allows estimating Δf and ROCOF, which model the three-phase system phase-angle evolution.

From a computational viewpoint, focusing on $\bar{X}_+$ estimation, the additional cost compared to a single-phase TF estimation is only due to the SV transformation applied to the three-phase signals. The parameter computation is identical since the same filter and the same formulas for frequency and ROCOF calculation are employed.

III. Tests and Results

The proposed SV-TF algorithm has been implemented in Matlab and tested by means of numerical simulations. A nominal frequency $f_0 = 50$ Hz has been considered, while a sampling frequency $f_s = 10$ kHz is used. TF filters have been designed by choosing $K = 2$ and three typical window lengths: two, four and six nominal cycles. Different lengths can help understanding the behavior of the algorithm that can be used to design PMU estimators for different applications.

A reporting rate equal to f_s has been considered, therefore synchrophasor, frequency and ROCOF are evaluated sample-by-sample. Accuracy is expressed in terms of total vector error (TVE) %, frequency error (FE) and ROCOF error (RFE) for synchrophasor, frequency and ROCOF estimations, respectively, as defined by [4]. In particular, maximum TVE, FE and RFE are considered when performance is assessed by applying some of the test signals proposed by [4]; results are compared with those obtained by employing conventional single-phase TF filters characterized by the same order and window lengths. A comparison with other estimation algorithms operating on SV signals, such those presented in [11], [12], which require specific configurations, is beyond the scope of this paper.

A. Impact of Broadband Noise

Measurements are typically affected by broadband noise due to quantization and disturbances. Therefore, it is interesting to assess the behavior of PMU algorithms by using positive sequence signals at the rated frequency with superimposed Gaussian noise. Maximum TVE, FE and RFE have been evaluated for both single-phase and SV-TF estimators with different signal to noise ratios (SNRs); only the TVEs are reported for the sake of brevity (Fig. 1), but FEs and RFEs show the same behavior. Errors are inversely proportional to the SNR and decrease with the window length. But, more important, the ratio between the TVE achieved by the single-phase TF estimator and that of the SV-TF method is $\sqrt{3}$. The reason is that SV transformation provides a coherent summation of the three single-phase signals, while noise adds incoherently.

B. Off-Nominal Frequency Test

Performance under off-nominal frequency conditions has been tested: a sinusoidal, positive sequence signal is applied, while its frequency is varied in the range $[45\,\text{Hz}, 55\,\text{Hz}]$. Errors

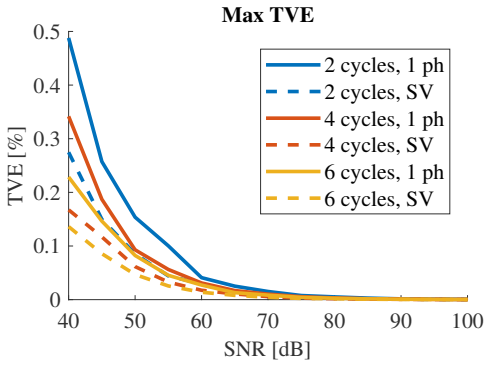

Fig. 1. Impact of broadband noise: maximum TVE achieved by conventional and SV TF approaches for different window lengths and SNRs.

are essentially due to two separate causes: the first one is the scalloping loss of the filters (also known as short-range leakage) that obviously increases as the difference between rated and actual frequency becomes larger. The second one is the spectral interference due to the image component (long-range leakage): also this effect becomes stronger by increasing the deviation between test frequency and its rated value; the reason is that the image component moves away from the zero(s) of the TF filter located at -f_0. Recalling (8), it becomes evident that the SV approach is completely immune to this effect: being the test signal three-phase balanced, its negative sequence component is zero.

Figs. 2 and 3 show that a longer window worsens synchrophasor and frequency estimation accuracy under off-nominal frequency. In fact, increasing the window length of a TF filter results in a narrower bandwidth, hence in higher scalloping loss. TVE values are extremely high for the six-cycle implementation ($3.9\,\%$ at $45\,\text{Hz}$ and $55\,\text{Hz}$) while they are well below $0.1\,\%$ when a two-cycle window is employed. In any case, from Fig. 2 it is evident that the SV approach results in considerably lower TVEs thanks to the cancellation of the image components that affect single-phase estimations. Frequency measurements are affected by large errors even when the two-cycle implementation is considered, as depicted by Fig. 3: it should be noticed that accuracies of the SV and of the single-phase estimations are very close, being the former just marginally better. The reason is that, in this case, performance is limited by the large scalloping loss. The opposite happens for the ROCOF estimation: Fig. 4 shows large RFE values when the single-phase approach is considered; such values are similar for the two, four and six cycle implementations. On the contrary, RFE achieved by using the SV-TF is negligible for all the considered window lengths. Being the actual ROCOF equal to zero, RFE of the single-phase estimation is solely due to the infiltration of the negative-frequency component, that on the contrary is completely canceled out by using a three-phase approach.

C. Amplitude and Phase Modulation Tests

In this test set, three-phase, positive-sequence signals modulated either in amplitude or in phase are applied [5]. The

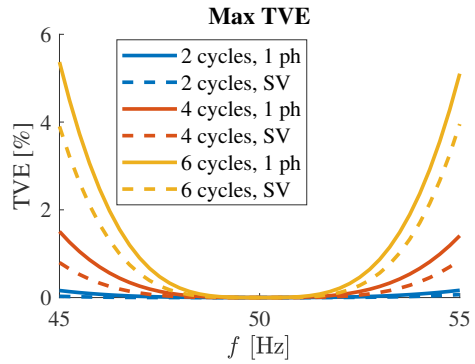

Fig. 2. Off-nominal frequency test: TVE achieved by conventional and SV TF approaches for different window lengths.

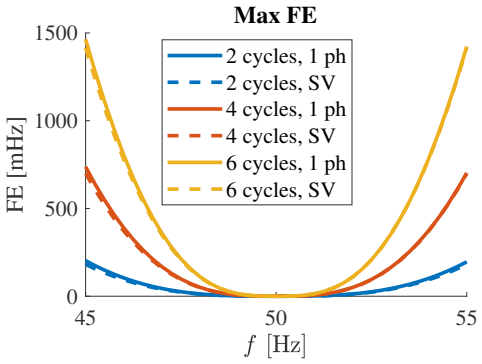

Fig. 3. Off-nominal frequency test: FE achieved by conventional and SV TF approaches for different window lengths.

generic expression of such signals is given by:

$$\boldsymbol{x}_{abc} = \sqrt{2}X\,(1+x_m)\cdot\Re\left(e^{j\varphi_m}\begin{bmatrix}1 & \bar{\alpha}^2 & \bar{\alpha}\end{bmatrix}^{\mathsf{T}}\right) \tag{23}$$

where X is the common rms magnitude and:

$$\begin{aligned} x_m &= k_x\cos\left(2\pi f_m t\right) \\ \varphi_m &= 2\pi f_0 t + k_a\cos\left(2\pi f_m t - \pi\right) \end{aligned} \tag{24}$$

with f_m as modulating frequency; as in [5], values up to 5 Hz have been employed during the tests. k_x and k_a represent the amplitude and phase modulation depths, respectively; the most severe conditions prescribed by [5] have been considered, thus $k_x = 0.1$, $k_a = 0$ during amplitude modulation tests and $k_x = 0$, $k_a = 0.1$ rad when dynamic performance in the presence of phase modulation is assessed.

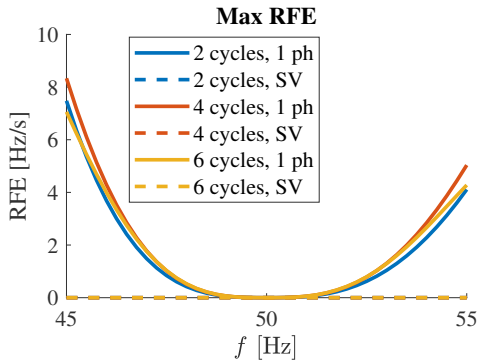

Fig. 4. Off-nominal frequency test: RFE achieved by conventional and SV TF approaches for different window lengths.

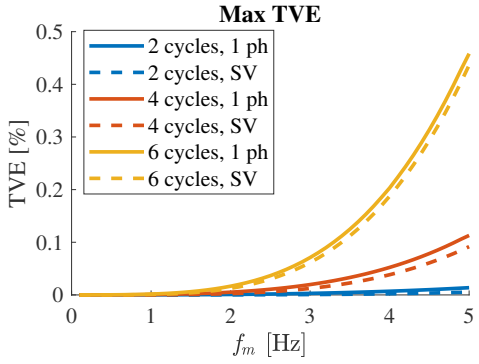

Fig. 5. Amplitude modulation test: TVE achieved by conventional and SV TF approaches for different window lengths.

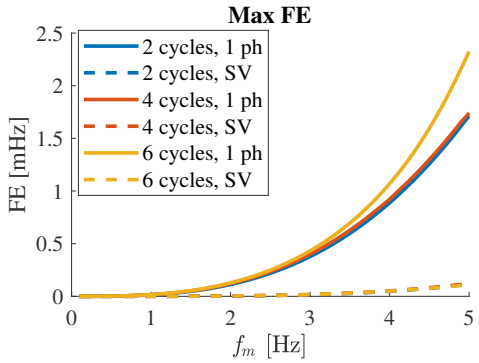

Fig. 6. Amplitude modulation test: FE achieved by conventional and SV TF approaches for different window lengths.

Figs. 5, 6 and 7 summarize the results for the amplitude modulation tests; errors increase monotonically with the modulating frequency. As expected, best results are achieved by using the shortest (two cycles) filters; furthermore, positive sequence estimations provided by SV-TF techniques are always characterized by lower errors with respect to the single-phase ones obtained by using the conventional TF filtering. Differences are fairly low for the synchrophasor estimation, since in this case errors are almost completely related to short-range leakage. Instead, the SV-TF algorithms show remarkable performance in frequency and ROCOF estimations, which are more heavily affected by the presence of negative-frequency terms. Considering $f_m = 5$ Hz, the single-phase TF algorithm achieves FE of about 2.3 mHz and 1.7 mHz for six-cycle and two-cycle filters; the SV-TF approach allows reducing these errors below 0.13 mHz. The single-phase estimator is characterized by RFEs between 0.59 Hz/s and 0.67 Hz/s for the three filter lengths while the SV-TF estimator results in RFEs below 0.031 Hz/s.

Finally, results obtained for the phase modulation tests are reported in Figs. 8 and 9. TVE values are not reported being them close to those achieved during the amplitude modulation tests: similar considerations apply. Things are completely different when looking at the frequency and ROCOF estimations. First of all, errors are much higher than in the amplitude modulation tests. Furthermore, the SV-TF does

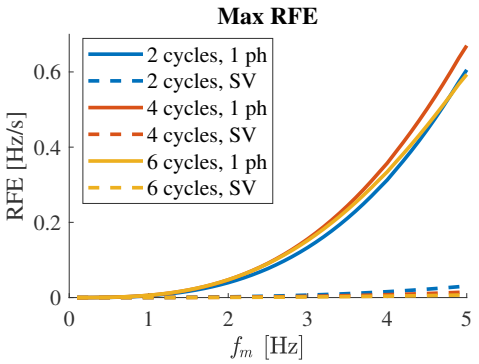

Fig. 7. Amplitude modulation test: RFE achieved by conventional and SV TF approaches for different window lengths.

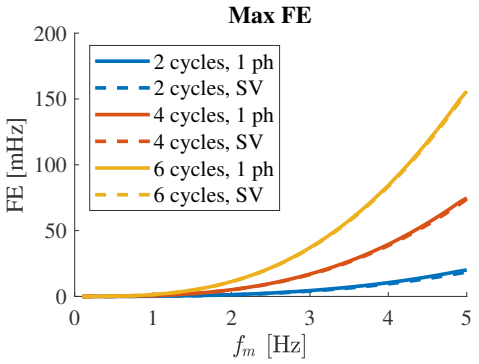

Fig. 8. Phase modulation test: FE achieved by conventional and SV TF approaches for different window lengths.

not result in dramatic performance improvement. The reason is that in this case both FE and RFE result from dynamic scalloping loss, which increases with the filter length. The error contribution due to the negative frequency components is not so important: the SV-TF achieves significantly better performance with respect to the single-phase approach only for the ROCOF estimation when considering a two-cycle filter. In this case, RFE is reduced from 0.73 Hz/s to 0.42 Hz/s.

Tests in the presence of harmonic and interharmonic disturbances, as prescribed in [4], have been also performed but results are not reported for the sake of brevity. Under these conditions, TVE, FE and RFE values strongly depend on the window length and, for a specific disturbance frequency, on the shape of the TF filter. Anyway, the SV approach allows reducing errors significantly thanks to the negative frequency cancellation.

IV. Conclusions

In this paper, the combination of two interesting approaches for PMU algorithm design in three-phase systems has been investigated. The TF filter has been used as a post-filtering stage after SV transformation to follow positive sequence synchrophasor, frequency and ROCOF dynamics. Algorithm performance has been assessed by simulating some of the typical test conditions proposed by the synchrophasor standard, thus showing that the SV approach is a valuable tool particularly when measurement errors are dominated by the infiltration of image frequency components. As expected,

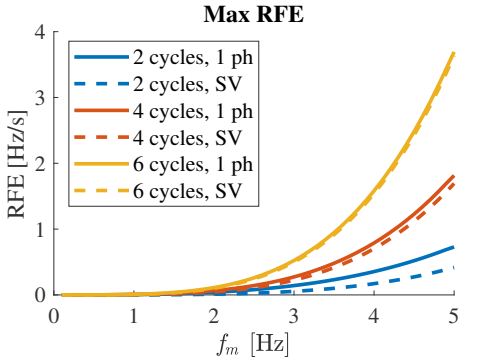

Fig. 9. Phase modulation test: RFE achieved by conventional and SV TF approaches for different window lengths.

window length plays a key role, therefore it is important to highlight that long time windows often conflict with the need to preserve the fundamental frequency component. In this regard, when there is no specific need to estimate single-phase phasors, the use of SV approach helps to reduce the length of observation intervals thanks to its capability to take advantage particularly of balanced or weakly unbalanced conditions.

References

[1] A. G. Phadke and J. S. Thorp, *Synchronized Phasor Measurements and Their Applications*. Springer Science, 2008.

[2] AA. VV., *Phasor Measurement Units and Wide Area Monitoring Systems*, 1st ed., A. Monti, C. Muscas, and F. Ponci, Eds. Academic Press, 2016.

[3] C. Muscas and P. A. Pegoraro, *Algorithms for synchrophasors, frequency, and rocof*, 1st ed. Eds. Elsevier, Academic Press, 2016, ch. ch. 3, p. 2151.

[4] *IEEE Standard for Synchrophasor Measurements for Power Systems*, IEEE IEEE Std C37.118.1-2011 (Revision of IEEE Std C37.118-2005), Dec. 2011.

[5] *IEEE Standard for Synchrophasor Measurements for Power Systems – Amendment 1: Modification of Selected Performance Requirements*, IEEE IEEE Std C37.118.1a-2014 (Amendment to IEEE Std C37.118.1-2011), Apr. 2014.

[6] J. A. de la O Serna, "Dynamic phasor estimates for power system oscillations," *IEEE Trans. Instrum. Meas.*, vol. 56, no. 5, pp. 1648–1657, Oct. 2007.

[7] W. Premerlani, B. Kasztenny, and M. Adamiak, "Development and implementation of a synchrophasor estimator capable of measurements under dynamic conditions," *IEEE Trans. Power Del.*, vol. 23, no. 1, pp. 109–123, Jan. 2008.

[8] R. K. Mai, Z. Y. He, L. Fu, B. Kirby, and Z. Q. Bo, "A dynamic synchrophasor estimation algorithm for online application," *IEEE Trans. Power Del.*, vol. 25, no. 2, pp. 570–578, Apr. 2010.

[9] D. Petri, D. Fontanelli, and D. Macii, "A frequency-domain algorithm for dynamic synchrophasor and frequency estimation," *IEEE Trans. Instrum. Meas.*, vol. 63, no. 10, pp. 2330–2340, Oct. 2014.

[10] P. Castello, J. Liu, C. Muscas, P. A. Pegoraro, F. Ponci, and A. Monti, "A fast and accurate PMU algorithm for P+M class measurement of synchrophasor and frequency," *IEEE Trans. Instrum. Meas.*, vol. 63, no. 12, pp. 2837–2845, Dec. 2014.

[11] S. Toscani and C. Muscas, "A space vector based approach for synchrophasor measurement," in *Instrum. and Meas. Technol. Conf. (I2MTC) Proc., 2014 IEEE Int.*, May 2014, pp. 257–261.

[12] S. Toscani, C. Muscas, and P. A. Pegoraro, "Design and performance prediction of space vector-based pmu algorithms," *IEEE Trans. Instrum. Meas.*, vol. 66, no. 3, pp. 394–404, Mar. 2017.

[13] R. Ferrero, P. A. Pegoraro, and S. Toscani, "Employment of interpolated DFT-based pmu algorithms in three-phase systems," in *Proc. IEEE Int. Work. on Appl. Meas. for Pow. Sys. (AMPS)*, Liverpool, UK, Sep. 2017.

[14] P. Castello, R. Ferrero, P. A. Pegoraro, and S. Toscani, "Effect of unbalance on positive-sequence synchrophasor, frequency, and ROCOF estimations," *IEEE Trans. Instrum. Meas.*, 2018, in press.